Int. J. Heat Mass Transfer. Vol. 35, No. 2, pp. 271–278, 1992
Printed in Great Britain

0017–9310/92 $5.00 + 0.00
Pergamon Press plc

Active nucleation site density and pool boiling heat transfer—an experimental study†

G. BARTHAU

Institut für Thermodynamik und Wärmetechnik, Universität Stuttgart, Pfaffenwaldring 6, D-7000 Stuttgart 80, Germany

(*Received* 25 *October* 1991)

Abstract—A novel optical method for measuring active nucleation site density is presented. The method has been used in pool boiling experiments with R114 on a horizontal tube and succeeded in measuring up to 5000 sites per cm^2. Heat transfer contribution of an individual active site is found to decrease with increasing pressure and is found to decrease strongly with increasing heat flux. The concept of area of influence of a bubble is discussed for the horizontal tube. Latent heat transfer is found to be significant even at lower heat fluxes.

1. INTRODUCTION

BY DEFINITION, nucleate boiling is characterized by the formation of vapour bubbles from fixed sites randomly distributed on a heater surface. Consequently, the number of these sites in a given area, the active nucleation site density, is one of the key parameters in nucleate boiling.

About 60 years ago, in one of the basic studies in boiling, Jakob and co-workers [1, 2] visually counted active nucleation sites in the low heat flux region of pool boiling water and found a linear relationship between active site density and heat flux.

Since then, many attempts have been made to count active sites, either by direct observation or by still or high-speed motion picture photography (e.g. see refs. [3–11]). However, these countings have been limited to low active site densities ($N/A < 100$ cm^{-2}) and to low heat fluxes, because at higher heat fluxes (and higher N/A) the large number of bubbles suspended in the boiling liquid obscured the view of the heater surface.

Gaertner and Westwater [12] developed a novel counting technique by superposing an electroplating process to nucleate boiling. They were able to identify up to 175 sites per cm^2 by subsequent counting of the pinholes in the electroplated layer.

Using electrically heated thin wires as heaters, Semeria [13] made the flow pattern of the rising bubbles two-dimensional and succeeded to measure more than 1000 bubble-columns per cm^2.

Kirby and Westwater [14] used a glass plate coated with a transparent, electrically-conducting material as a resistance heater and were able to count up to 630 sites per cm^2 by high-speed motion picture photography from below.

With a miniature void-detection probe, operated within a small distance above a heater plate, Iida and Kobayasi [15] located up to 150 sites per cm^2.

Myers and co-workers [16, 17] used electrically heated thin stainless steel sheets as heaters and recorded the temperature patterns on the underside of the sheets, either by liquid crystal coatings or with a high-speed infrared camera, thus identifying the active sites on the upper side.

Despite their merits, these methods have the disadvantage of being limited to either special types of fluids or to special types of heaters.

In the present study, a simple optical method for counting active nucleation sites has been developed which is suitable for one of the most common type of test heaters, the plain horizontal tube, and which is hopefully suitable for all transparent liquids.

This method has been used to measure active site density in pool boiling of R114 at pressures of $p = 1.50$, 1.91 and 2.47 bar and heat fluxes up to $q = 7 \times 10^4$ W m^{-2}.

By simultaneous measurement of bubble parameters (departure diameter and frequency), heat transfer and active site density, the contribution of an individual site to heat transfer is evaluated, using a minimum of theoretical assumptions.

2. MEASUREMENT METHOD FOR ACTIVE NUCLEATION SITE DENSITY

The principle of the method presented is simple and it is rather astonishing that, as far as I know, its use has not been reported previously.

When a boiling surface is observed in *directly reflected* light from a (small) light source, the image of the detached (and moving) bubbles becomes 'smeared'. On the other hand, the bubbles still growing from an active site, being fixed to the surface, 'shade' the ambience of the site, marking them-

† Dedicated to Prof. Dr.-Ing. E. Hahne on the occasion of his 60th birthday.

NOMENCLATURE

A	area
d	tube diameter
D	diameter of area of influence
D_d	departure diameter of bubble
f	frequency
g	gravitational acceleration
Gr^*	modified Grashof number
Δh_v	latent heat of evaporation
N	total number of active nucleation sites
N_b	average number of active nucleation sites at a given instant
p	pressure
p_{cr}	critical pressure
Pr	Prandtl number
q	heat flux
q_c	natural convection heat flux
q_c^*	natural convection heat flux in presence of bubbles
Q	heat flow
Q_b	heat flow by bubbles
Q_c^*	natural convection heat flow in presence of bubbles
r	critical radius
s	average active nucleation site spacing
ΔT	excess temperature
T_s	(thermodynamic) saturation temperature.

Greek symbols

α	heat transfer coefficient
β	thermal coefficient of expansion
ν	kinematic viscosity
ρ_m	average density
ρ_∞	reference density
ρ'	density of saturated liquid
ρ''	density of saturated vapour
σ	surface tension.

selves as dark spots on the heater surface (Fig. 1). For the horizontal tube and horizontal observation direction, the vertical flank of the tube is a preferable observation region because the detached bubbles move vertically to the observation direction and the bubbly layer is relatively thin.

The effect described can be observed even with the naked eye using a pocket lamp and is most pronounced when the angle between the incident light and the direction of observation is small.

To count the dark spots, a small measuring telescope (operating distance 300–400 mm, magnification 12×) equipped with a graduated plate is used. Directly behind the eye piece of the telescope a video-camera with a zoom lens is placed, resulting in an overall magnification of up to 200× on the video-screen. The dark spots are marked on a transparent foil fixed on the video-screen and thus can be counted easily. The dimensions of the measurement area are given by the graduated plate of the telescope. Depending on active site density, different measurement areas (different magnifications by adjusting the zoom lens) are used.

When the total number of active sites on the test tube is less than 100 ($N/A < 2$ cm^{-2}) direct counts are taken.

For taking the photographs shown in Fig. 1, the video-camera was replaced by a reflex camera. The exposure time was 0.75 s. Position 0 on the scale corresponds to the axis and position 8 to the lower contour of the test tube.

3. EXPERIMENTAL SET-UP AND PROCEDURE

A sketch of the experimental arrangement is shown in Fig. 2. The experiments were performed in a cylindrical stainless steel vessel (i.d. 300 mm, length 170 mm) equipped with sight glasses in the front and the rear wall. A detailed description of the apparatus is given by Gorenflo *et al.* [18].

In order to develop the active nucleation site counting method, the boiling apparatus had to be freely accessible from the outside. For this reason the apparatus was operated in a temperature controlled room, the air temperature being adjusted to the saturation temperature of the boiling liquid to within ±0.2 K.

The test tube† is an electrically heated, horizontal copper cylinder of 8 mm o.d. and 200 mm length (for constructive details see ref. [18]). The surface of the tube has been prepared by grinding with emery paper in the axial direction (roughness parameters according to German standards: $R_a = 0.52$ μm; $R_p = 1.48$ μm; $R_z = 1.99$ μm).

After the first installation of the tube in the thoroughly cleaned boiling apparatus and condensing R114 into the evacuated vessel, the heater surface was only in contact with the refrigerant. For the experiments reported here, the surface seems to have reached physico-chemical equilibrium for the boiling process with the test liquid.

The excess temperature of the heated wall is measured in the middle of the tube with eight NiCr–Ni thermocouples, equally distributed around the circumference. The reference temperature is measured

† The test tube was provided by Professor Gorenflo, LWK University Paderborn, in order to perform pool boiling comparison experiments with R114. The author feels very indebted to Professor Gorenflo to let him work with this tube.

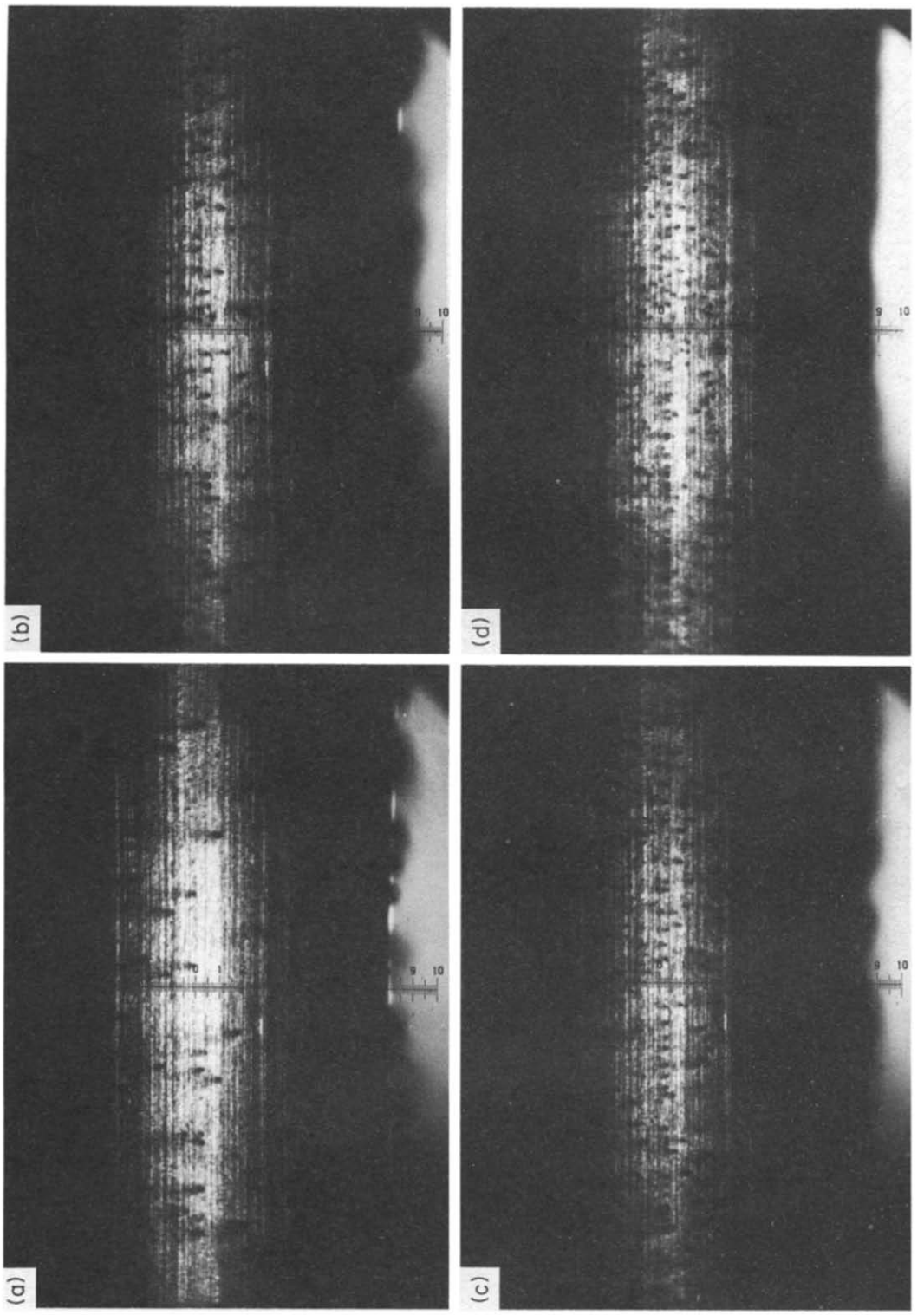

FIG. 1. Photographs of active nucleation sites ($p = 1.91$ bar): (a) $q = 10\,000$ W m^{-2}; (b) $q = 20\,000$ W m^{-2}; (c) $q = 30\,000$ W m^{-2}; (d) $q = 40\,000$ W m^{-2}.

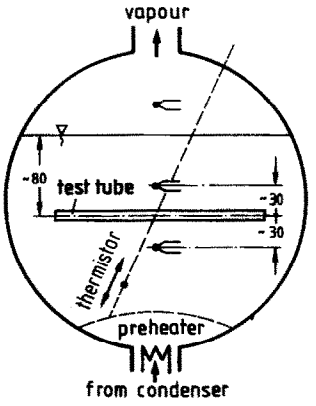

FIG. 2. Experimental arrangement.

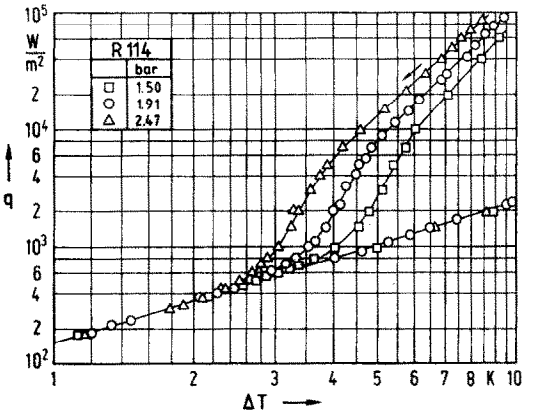

FIG. 3. Heat flux vs excess temperature for different pressures.

with a thermocouple immersed in the test liquid, approximately 30 mm below the test tube. The excess temperature ΔT of the heater surface is calculated as the arithmetic mean of the eight signals, corrected for the radial temperature drop between thermocouples and surface. Accuracy of excess temperature measurement is estimated to be better than 0.01 K for $q < 3000$ W m^{-2}.

The heat flow Q is calculated with the current, measured using a precision resistor and the voltage drop of the resistance heater in the test tube. Accuracy of the heat flux q, corrected for the heat losses at the ends of the test tube, is estimated to be better than 1%.

The liquid and vapour temperature are measured respectively with three NiCr–Ni thermocouples.

To check for vertical temperature gradients in the test liquid, a high resolution thermistor is arranged in a thin-walled stainless steel tube 45 mm behind the test tube. It can be shifted in the vertical direction from outside the boiling vessel.

All boiling experiments were run with decreasing heat flux. Some of the natural convection runs were performed with increasing heat flux.

For boiling runs with $q > 3000$ W m^{-2}, the power of the preheater was adjusted to produce a minimum of bubbles rising through the test liquid.

Boiling runs with $q < 3000$ W m^{-2} and all natural convection runs were performed with the preheater being switched off. In these runs, the saturation temperature of the test liquid in the boiling vessel was kept about 0.1 K below the average ambient temperature.

Bubble departure diameter and frequency were measured using the telescope and a stroboscope. Accuracy of the diameter measurements is estimated to be better than ± 0.1 mm.

4. EXPERIMENTAL RESULTS

4.1. *Heat transfer*

Heat transfer results are shown in Fig. 3 in a double logarithmic plot of the heat flux q over the excess temperature ΔT.

For the sake of higher resolution in graphical presentation, the data for the low heat flux region are plotted in Fig. 4 as differences of heat fluxes with and without bubble formation $(q-q_c)$ vs ΔT. The numbers near the symbols in Fig. 4 give the total (direct counted) number of active sites on the surface of the test tube.

4.2. *Bubble parameters*

For $p = 1.91$ bar, the measured departure diameters D_d and frequencies f of bubbles, depending on the circumferential position of active sites, are shown in Fig. 5. The frequencies reported are averaged values, the observed fluctuations being $\pm 10\%$. The data have been taken at a heat flux $q \approx 1500$ W m^{-2} and refer to individual, undisturbed bubbles, not influenced by their neighbours.

For the lower pressure ($p = 1.50$ bar) the departure diameters generally were found to be somewhat higher ($D_d \approx 0.35$ mm on the flank of the tube) and the frequencies to be somewhat lower.

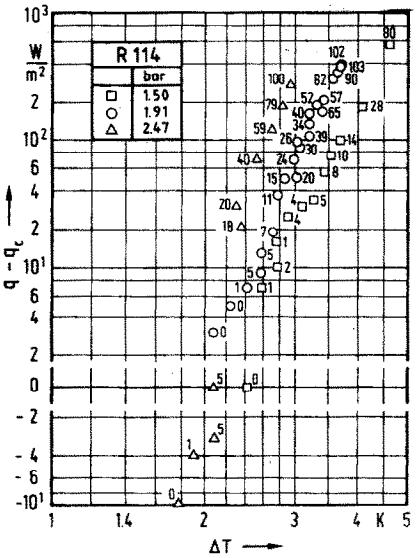

FIG. 4. Boiling component of heat flux vs excess temperature for different pressures; number of active sites.

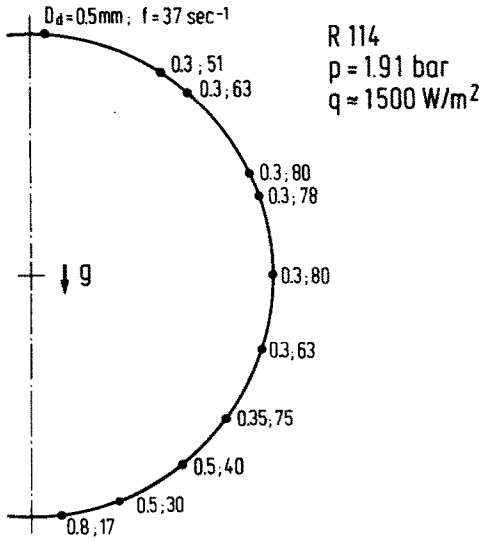

FIG. 5. Departure diameter and frequency of bubbles depending on circumferential position.

For $p = 2.47$ bar, the corresponding departure diameter was $D_d \approx 0.25$ mm, the frequencies being somewhat higher than for $p = 1.91$ bar.

Generally, a small increase of departure diameter *and* of frequency has been observed with increasing heat flux, the frequency fluctuations becoming larger at higher heat fluxes.

Bubbles nucleating by 'site seeding' in the wake of primary bubbles clearly showed smaller departure diameters and highly irregular frequencies.

4.3. *Active nucleation site density*

Measured active site densities are shown in Fig. 6 in a double logarithmic plot as N/A vs heat flux q.

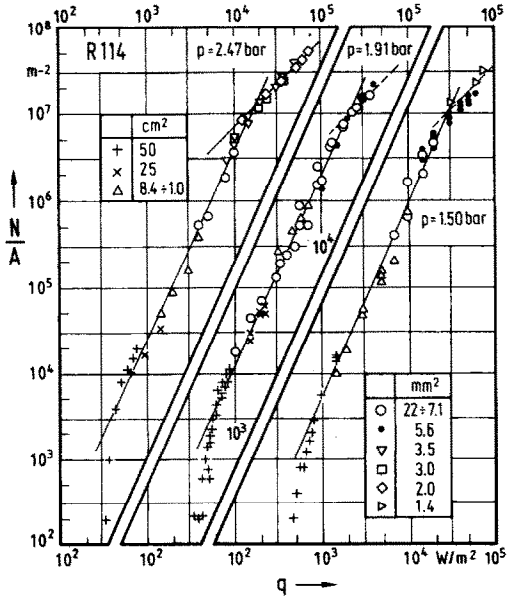

FIG. 6. Active nucleation site density vs heat flux for different pressures.

Different symbols are used to characterize different measurement areas.

At low active site densities ($N/A < 2 \times 10^4$ m^{-2}), sites behaved very stably, showing a continuous emission of bubbles, even over periods of days.

At high active site densities ($N/A > 10^7$ m^{-2}) seldom a really stable active site could be observed. Neighbouring sites showed an intermittent behaviour, giving the impression of 'competing for the heat' or 'blowing-off' each other.

As can be seen from the photographs in Fig. 1, the active sites are not randomly distributed over the surface of the test tube. Particular axial grooves are densely populated, whereas others are nearly bare.

5. EVALUATION OF DATA AND DISCUSSION

5.1. *Heat transfer*

For convenience, in Fig. 7 the heat transfer data are replotted as heat transfer coefficient α vs heat flux q. In the range $5000 < q < 10000$ W m^{-2} a small but clearly distinguishable discontinuity in the slopes of the α, q curves can be observed.

A re-examination of numerous precise pool boiling data (e.g. see ref. [19]) reveals that such a break in the boiling curve is sometimes exhibited by the experimental data, but is often masked by the straight-line fitting in double logarithmic diagrams.

With reference to Nishikawa *et al.*'s data for the tilted plate [20], which show a strong influence of inclination on nucleate boiling heat transfer in the lower heat flux region, it seems rather logical that a horizontal tube, which can be seen as assembled by differently inclined plate elements, exhibits a similar behaviour.

5.2. *Active nucleation site density*

As follows from Fig. 6, the experimental data for different areas of measurement overlap fairly well, indicating that for high active site densities even measurement areas of a few square millimetres provide representative results.

The experimental data for the different pressures investigated exhibit the same characteristic be-

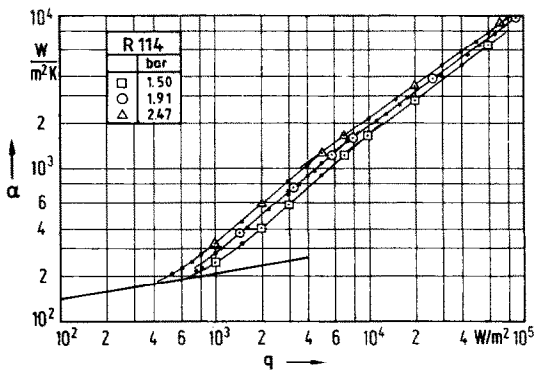

FIG. 7. Heat transfer coefficient vs heat flux for different pressures.

haviour. In the range of three orders of magnitude ($10^4 < N/A < 10^7$ m^{-2}), N/A increases nearly quadratically with heat flux. The deviations for the lowest active site densities are felt to be due to a non-representative measurement area ($N/A = 2 \times 10^3$ m^{-2} corresponding to 10 active sites on the test tube). At $N/A \approx 10^7$ m^{-2} the (nearly) quadratic relation between N/A and q begins to change to a linear one, being most evident for the data for $p = 2.47$ bar.

The nearly quadratic increase of N/A with q of the present data is in close agreement with the data obtained in refs. [5, 12, 15]. The tendency of flattening of the N/A, q curves at higher N/A can be found also in the data of refs. [10, 13, 21].

In Fig. 8 the data of the present study are plotted in a double logarithmic diagram as cumulative active site density vs the critical radius r, with

$$r = \frac{2\sigma T_s}{\Delta h_v \rho'' \Delta T} \tag{1}$$

As can be seen, the data fit well with a power law distribution, originally proposed by Brown [22].

Siebert [11], using a current theoretical model, calculated N/A from boiling heat transfer experiments with R114, performed on a similar test tube with similar surface preparation as used in the present study. The heat transfer data from both studies compare well. However, the calculated active site densities for higher heat fluxes differ by more than an order of magnitude from the measured ones of the present study. Therefore, transient conduction boiling models should be re-examined.

5.3. *Heat transfer contribution of an individual active site*

The measured total heat flow rate Q in pool boiling can be divided into a heat flow, Q_c^*, by natural convection and a heat flow, Q_b, by bubble formation.

With D the diameter of the area of influence of a bubble, N_b the average number of active sites at a given instant and q_c^* the natural convection heat flux in the presence of bubbles one obtains

$$Q_b = Q - Q_c^* = q \times A - q_c^* \cdot \left(A - N_b \frac{\pi}{4} D^2 \right)$$

$$\text{for} \quad A > (N_b \cdot \pi/4 \cdot D^2) \tag{2}$$

and for an individual active site

$$\frac{Q_b}{N} = \frac{A}{N}\left[q - q_c^* \cdot \left(1 - \frac{N_b}{A} \cdot \frac{\pi}{4} \cdot D^2 \right) \right]. \tag{3}$$

In order to calculate Q_b/N according to equation (3), the following assumptions are made:

(i) the measured excess temperature ΔT is representative for the total surface of the test tube
(ii) $D = 2 \cdot D_b$
(iii) $q_c^* = q_c$
(iv) $N_b = N$

resulting in

$$\frac{Q_b}{N} = \frac{A}{N}\left[q - q_c \cdot \left(1 - \frac{N}{A} \pi D_b^2 \right) \right]. \tag{4}$$

According to equation (4), Q_b/N is evaluated using

$D_b = 0.35$ mm for $p = 1.50$ bar

$D_b = 0.30$ mm for $p = 1.91$ bar

$D_b = 0.25$ mm for $p = 2.47$ bar.

The results are plotted in Fig. 9 vs the average active site spacing s, being taken as

$$s = (A/N)^{0.5} \tag{5}$$

as proposed by Zuber [23].

Assumption (i) may have some influence on the accuracy of Q_b/N for large spacings ($s > 10$ mm) where the measured excess temperature may differ from the average between the excess temperature of the (extended) natural convection areas and the excess temperature of the (small) areas of influence of bubbles.

To check the sensitivity of Q_b/N as concerns

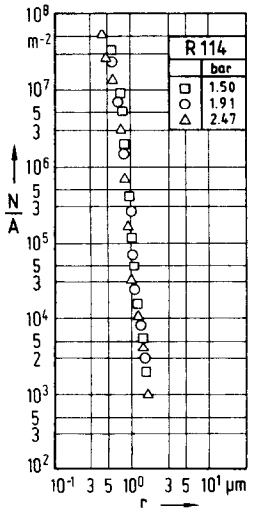

FIG. 8. Cumulative active nucleation site density vs critical radius.

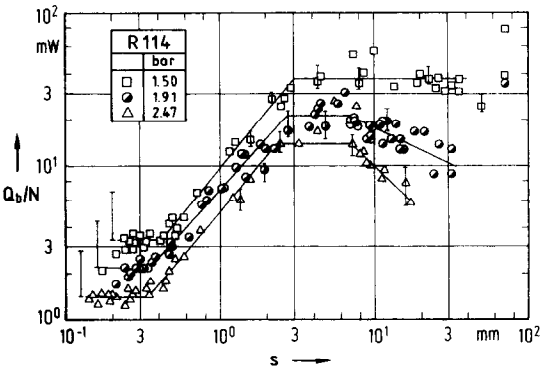

FIG. 9. Heat removed by an individual active site vs average active site spacing.

assumption (ii), equation (4) is evaluated also using $D = 10 \times D_b$ as a conservative upper limit. For the relevant range

$$(N_b/A \cdot \pi/4 \cdot D^2) < 1$$

the results are shown as upper error bars in Fig. 9, indicating a minor influence on Q_b/N.

To check for the influence of assumption (iii), the natural convection component q_c^* is evaluated using a modified Gr, Gr^*, proposed by Zuber [23]

$$Gr^* = \frac{g \cdot d^3}{\nu^2} \cdot \frac{\rho_\infty - \rho_m}{\rho_\infty} \quad (6)$$

with

$$\frac{\rho_\infty - \rho_m}{\rho_\infty} = \beta \cdot \Delta T + \left[\frac{N}{A} \cdot \frac{\pi}{6} \cdot D_d^2 \cdot \frac{\rho' - \rho''}{\rho'}\right]. \quad (7)$$

The results are shown in Fig. 9 as lower error bars, also indicating a minor influence on Q_b/N.

Since $N_b/N \geqslant 0.5$ (as will be discussed later), the influence of assumption (iv) on the results is much smaller than the influence due to assumption (ii) (compare equation (3)) and therefore can be neglected.

A comparison of the total number of active sites N measured as described, with data for N_b, taken from photographs (exposure times 1/10 to 1 s), gives a ratio $N_b/N \geqslant 0.5$, showing no systematic dependence from exposure time. For subcooled pool boiling of water Judd and Merte [24] also found $N_b/N \approx 1/2$.

For the present data the estimated range for Q_b/N_b (based on the average population density N_b/A instead of on the active site density N/A) for higher heat fluxes is shown by the bars in the left corner of Fig. 9.

As stated in Section 4.3, the individual sites behave very stably at low active site densities ($N_b/N = 1$), and hence for low heat fluxes Q_b/N_b will approach Q_b/N.

5.4. *Discussion*

Gaertner and Westwater [12] have found the contribution to the total heat flux of an individual site to diminish with increasing heat flux (decreasing average spacing between active sites). The results of the present study confirm this finding.

Not taking into account, at this stage, the data for $s > 7$ mm, Q_b/N for the different pressures investigated exhibits a uniform characteristic behaviour. At spacings $s \approx (7 \text{ to } 10) \cdot D_d$, the heat removed by an individual site begins to decrease and seems to stabilize on a lower level at $s \approx 1D_d$.

It was a very unexpected result that even at spacings of $s \approx (7 \text{ to } 10) \cdot D_d$ some interference between the areas of influence seems to occur.

On the other hand, it is questionable whether the customary approach $D = 2D_d$ (proposed by Han and Griffith [6] for the horizontal plate) can be accepted unconstrained for the horizontal tube. If the change in the slope of heat transfer coefficient α vs heat flux q (discussed in Section 5.1) is interpreted as the beginning of overlap of areas of influence, an average diameter of the area of influence $D \approx 3D_d$ for the horizontal tube would result from the present data.

An interaction of bubbles at even higher spacings at low heat fluxes might be explained by taking into account an extended area of influence due to sliding bubbles as proposed by Hahne *et al.* [25] for finned tubes.

In the range $s \approx 1D_d$, the bubbles obviously come into direct lateral contact on the heater surface. It is tempting to use this 'lower knee' in the $(Q_b/N), s$ curve to define an average departure diameter for the bubbles.

A rough calculation, assuming the departure frequencies measured in the isolated bubble region to hold also in the crowded bubble region, reveals that latent heat transport is significant in the range $s \approx 1D_d$.

6. SUMMARY

The results of the present study can be summarized as follows:

For R114, boiling on a horizontal copper tube at pressures $1.50 \leqslant p \leqslant 2.47$ bar $(0.05 \leqslant p/p_{cr} \leqslant 0.08)$

- the contribution of an individual active site to boiling heat flux decreases with increasing pressure,
- the contribution of an individual active site to boiling heat flux decreases strongly with increasing excess temperature (increasing heat flux) and stabilizes on a lower level,
- the average spacing between active sites becomes equivalent to bubble departure diameter at heat fluxes of about 10% of the critical heat flux, and
- the latent heat transport is already significant at lower heat fluxes.

Therefore, current models of nucleate boiling should be re-examined.

REFERENCES

1. M. Jakob und W. Fritz, Versuche über den Verdampfungsvorgang, *Forsch. Ing. Wes.* **2**, 435–447 (1931).
2. M. Jakob and W. Linke, Der Wärmeübergang von einer waagerechten Platte an siedendes Wasser, *Forsch. Ing. Wes.* **4**, 75–81 (1933).
3. C. Corty, Surface variables in boiling, Ph.D. Thesis, University of Michigan (1951).
4. K. Nishikawa, Studies on heat transfer in nucleate boiling, *Mem. Fac. Engng, Kyushu Univ.* **16**, 1–28 (1956).
5. H. M. Kurihara and J. E. Myers, The effect of superheat and surface roughness on boiling coefficients, *A.I.Ch.E. Jl* **6**, 83–91 (1960).
6. C. Y. Han and P. Griffith, The mechanism of heat transfer in nucleate pool boiling, *Int. J. Heat Mass Transfer* **8**, 887–914 (1965).
7. A. P. Hatton and I. S. Hall, Photographic study of boiling on prepared surfaces, *Proc. 3rd Int. Heat Transfer Conf.*, Chicago, Vol. 4, pp. 24–37 (1966).
8. M. Güttinger, Die Verbesserung des Wärmeübergangs bei der Verdampfung in überfluteten Rohrbündel-

verdampfern, *4th Int. Heat Transfer Conf.*, Paris-Versailles, Vol. 1, HE 2.4 (1970).
9. K. Cornwell and R. D. Brown, Boiling surface topography, *6th Int. Heat Transfer Conf.*, Toronto, Vol. 1, pp. 157–161 (1978).
10. S. Faggiani, P. Galbiati and W. Grassi, Active site density, bubble frequency and departure diameter in water and Freon 113 boiling on chemically etched surfaces, *La Termotecnica* **35,** 511–519 (1981).
11. M. Siebert, Untersuchung zum Einfluß des Wandmaterials und des Rohrdurchmessers auf den Wärmeübergang von horizontalen Rohren an siedende Flüssigkeiten, Diss. Univ. Karlsruhe (1987).
12. R. F. Gaertner and J. W. Westwater, Population of active sites in nucleate boiling heat transfer, *Chem. Engng Prog. Symp. Ser. No. 30* **56,** 39–48 (1960).
13. R. L. Semeria, An experimental study of the characteristics of vapour bubbles, Symp. Two-phase Fluid Flow, Paper 7, London (1962).
14. D. B. Kirby and J. W. Westwater, Bubble and vapor behavior on a heated horizontal plate during pool boiling near burnout, *Chem. Engng Prog. Symp. Ser. No. 57* **61,** 238–248 (1965).
15. Y. Iida and K. Kobayasi, An experimental investigation on the mechanism of pool boiling phenomena by a probe method, *4th Int. Heat Transfer Conf.*, Paris-Versailles, Vol. 5, B1.3 (1970).
16. T. Raad and J. E. Myers, Nucleation studies in pool boiling on thin plates using liquid crystals, *A.I.Ch.E. Jl* **17,** 1260–1261 (1971).
17. J. E. Sgheiza and J. E. Myers, Behavior of nucleation sites in pool boiling, *A.I.Ch.E. Jl* **31,** 1605–1613 (1985).
18. D. Gorenflo, J. Goetz und K. Bier, Vorschlag für eine Standard-Apparatur zur Messung des Wärmeübergangs beim Blasensieden, *Wärme Stoffubertrag.* **16,** 69–78 (1982).
19. VDI-Wärmeatlas, Berechnungsblätter für den Wärmeübergang. Ha 1, 5. Auflage. VDI-Verl. (1988).
20. K. Nishikawa, Y. Fujita, S. Uchida and H. Ohta, Effect of surface configuration on nucleate boiling heat transfer, *Int. J. Heat Mass Transfer* **27,** 1559–1571 (1984).
21. C. J. Rallis and H. H. Jawurek, Latent heat transport in saturated nucleate boiling, *Int. J. Heat Mass Transfer* **7,** 1051–1068 (1964).
22. W. T. Brown, Jr., Study of flow surface boiling, Ph.D. Thesis, Mech. Engng Dept., M.I.T. (1967).
23. N. Zuber, Nucleate boiling. The region of isolated bubbles and the similarity with natural convection, *Int. J. Heat Mass Transfer* **6,** 53–78 (1963).
24. R. L. Judd and H. Merte, Influence of acceleration on subcooled nucleate pool boiling, *4th Int. Heat Transfer Conf.*, Paris-Versailles, Vol. 6, B8.7 (1970).
25. E. Hahne, Chen Qiu-Rong and R. Windisch, Pool boiling heat transfer on finned tubes—an experimental and theoretical study, *Int. J. Heat Mass Transfer* **34,** 2071–2079 (1991).

DENSITE DE SITES ACTIFS DE NUCLEATION ET TRANSFERT THERMIQUE D'EBULLITION—UNE ETUDE EXPERIMENTALE

Résumé—On présente une nouvelle méthode optique pour mesurer la densité de sites actifs de nucléation. Elle est utilisée dans des expériences d'ébullition nucléée avec R 114 sur un tube horizontal et elle permet de mesurer jusqu'à 5000 sites par cm^2. La contribution d'un seul site actif au transfert thermique diminue quand la pression augmente et elle décroît fortement quand le flux thermique croît. On discute pour le tube horizontal, le concept d'aire d'influence d'une bulle. Le transfert de chaleur latente est important même aux plus faibles flux thermiques.

AKTIVE KEIMSTELLENDICHTE UND WÄRMEÜBERGANG BEIM BEHÄLTERSIEDEN—EINE EXPERIMENTELLE UNTERSUCHUNG

Zusammenfassung—Ein neues optisches Verfahren zur Bestimmung der aktiven Keimstellendichte wird beschrieben. Das Verfahren wurde beim Behältersieden von R114 am waagerechten Rohr eingesetzt; dabei konnten bis zu 5000 aktive Keimstellen/cm^2 gezählt werden. Der Beitrag einer einzelnen aktiven Keimstelle zum Wärmetransport nimmt mit steigenden Druck und noch stärker mit steigender Wärmestromdichte ab. Das Konzept des Einflußbereichs einer Blase wird für den Fall des waagerechten Rohres diskutiert. Eine Abschätzung des Latentwärme-Anteils ergibt schon für kleine Wärmestromdichten einen erheblichen Beitrag zum Wärmetransport.

ПЛОТНОСТЬ ЦЕНТРОВ НУКЛЕАЦИИ И ТЕПЛОПЕРЕНОС ПРИ КИПЕНИИ В БОЛЬШОМ ОБЪЕМЕ. ЭКСПЕРИМЕНТАЛЬНОЕ ИССЛЕДОВАНИЕ

Аннотация—Предложен новый оптический метод измерения плотности центров нуклеации. Метод использовался в экспериментах по пленочному кипению хладагента R114 на горизонтальной трубе, в измерениях фиксировалась до 5000 центров на $см^2$. Найдено, что вклад от отдельного центра в теплоперенос уменьшается с ростом давления и особенно заметно убывает с увеличением теплового потока. Обсуждается концепция зоны влияния пузырька для случая горизонтальной трубы. Найдено, что скрытый теплоперенос является существенным даже при малых тепловых потоках.